Proceedings of the 2021 Winter Simulation Conference
S. Kim, B. Feng, K. Smith, S. Masoud, Z. Zheng, C. Szabo, and M. Loper, eds.

MULTI-FIDELITY MODELING FOR THE DESIGN OF A MARITIME ENVIRONMENTAL SURVEY NETWORK UTILIZING UNMANNED UNDERWATER VEHICLES

Danielle F. Morey
Zelda B. Zabinsky

Industrial and Systems Engineering Department
University of Washington
Seattle, WA 98195-2650, U.S.A.

Cherry Wakayama
Randall Plate

Intelligence, Surveillance
and Reconnaissance Department
Naval Information Warfare Center Pacific
San Diego, CA 92152-5001, U.S.A.

ABSTRACT

New maritime operational concepts are being considered for future network topologies that are efficient and reliable in underwater domains where the design of networking is challenging due to the harshness of the environment. Various communication and network simulation tools exist to model scenarios of interest and evaluate metrics of interest, e.g., latency, throughput and reliability, for high-fidelity evaluations. However, the computation time required for high-fidelity simulation is extensive for evaluating many network topologies associated with topology optimization. Thus we develop low-fidelity models to explore many network topologies and identify a few Pareto optimal configurations to evaluate with the high-fidelity simulation. In this paper, we demonstrate a multi-fidelity topology optimization methodology for maritime environmental survey operations involving multiple unmanned underwater vehicles. The low-fidelity models developed for this maritime operation scenario are able to accurately identify the intuitive optimal solution based on multiple objectives, which are then validated by high-fidelity simulations.

1 INTRODUCTION

With the maturity of networking and autonomous unmanned technologies, new applications for networked sensors and assets in underwater domains are emerging for public, commercial and defense services. Wireless sensor networks are being considered in the underwater domain to monitor the health of marine environments (Vasilescu et al. 2005). Unmanned underwater vehicles (UUVs) are being used by the oil and gas industry to map the seafloor prior to construction of subsea infrastructure (Zwolak et al. 2017). Key technologies in UUVs, sensors, underwater communication networks and autonomous behavior are driving new operational concepts for performing various undersea Intelligence, Surveillance and Reconnaissance (ISR) mission tasks (Fletcher 2000).

Underwater operations are generally costly, challenging and complex because of the harsh underwater environment, limited power supply and limited underwater communication channels. Considerable work, resources and careful planning are required to deploy and maintain sensors and assets to perform underwater operations (LiVecchi et al. 2019). Addressing these challenges, our work focuses on developing a modeling methodology to evaluate and optimize different design topologies for deploying multiple sensors and assets that perform specific operational missions. In particular our model development emphasizes the communication and networking aspect of maritime topologies that can support various data exchange requirements, such as data volume, data timeliness, energy usage and delivery reliability. There is considerable literature concerning routing and methods of path planning (Echeveste et al. 2021; Zhang and Fei 2007). This work aims to expand the literature by focusing on topology design under the assumption of fixed routing.

978-1-6654-3311-2/21/$31.00 ©2021 IEEE

Without loss of generality and for ease of reference, we represent an end-to-end maritime mission system as a control system composed of observation, decision and action layers with each layer composed of independent nodes or a network of distributed nodes which perform specific roles: observation nodes collect data, decision nodes offer centralized or decentralized decision capabilities, and action nodes perform actions for timely implementation. Nodes may interact with other nodes in the same layer and/or across layers depending on the decision and networking topologies. The data are sent to nodes in the decision layer via available communication and network (C&N) links for decision making. This paper focuses on the topology design of a communication network involving mobile observation nodes (UUVs) for delivering a large amount of data from observation layer to decision layer.

Topology optimization for a complex system of systems can be viewed as a black-box global optimization problem where high-computation high-fidelity simulation models are often required to perform evaluation of measures of performance (Fu 2015; Kang et al. 2017; Linz et al. 2017). However, these high-fidelity models are too computationally expensive to iteratively run over a parameter space in order to find optimal configurations. Thus, our approach to topology optimization is based on multi-fidelity modeling and simulation, in which low-computation low-fidelity models that are capable of being solved efficiently are first constructed to provide quick insight and information on topology configurations. Guided by the solutions of low-fidelity models, a reasonable number of topology configurations are systematically selected for further evaluation using high-fidelity simulation models. These limited high-fidelity evaluations are then used to validate the low-fidelity models in producing trends on performance measures that are fairly consistent with varying topology configurations. In future work, we plan to develop a feedback scheme which uses observed discrepancy measures to calibrate low-fidelity models for improved accuracy.

In this work we explore the topology configurations for a maritime environment survey operation involving multiple UUVs collecting large volumes of data in an operational area and delivering the data to a processing or decision center, which is referred to as a depot. The design variables involve determining the optimal topology configuration based on the number of UUVs to deploy and the number of location nodes to be visited by each UUV. To address failure probability associated with maritime systems and underwater operations, delivery reliability, in the form of redundancy in coverage, is also considered in the construction of topology configurations. From a communication and networking perspective, the interested measures of performance include delivery delay, location node revisit rate and delivery reliability in addition to cost (number of UUVs) and energy usage.

It is important to clearly outline the differences between the low-fidelity and high-fidelity models in this paper. Our low-fidelity models capture measures of performance in an aggregated view by combining individual details into group representations under simplifying assumptions. Instead of characterizing individual UUV trips and paths, all UUV trips and paths are represented using single common metrics. For example, a fixed round-trip duration and energy usage are used for all UUVs without detailed path planning for each UUV. Weighted revisit time is defined to capture the node revisit rate, and expected number of unsuccessful deliveries (the number of data collection nodes that fail to have data successfully transmitted to the depot) is computed to capture delivery reliability under the simplifying assumptions that UUV trips are independent and the data collection, transporting, and transmission events are independent.

On the other hand, our high-fidelity model implements direct simulation. A detailed scenario with specific node locations, UUV movements and behaviors, and data transfer over specified communication links are programmed to execute the scenario for a specified mission duration. A fixed path must be explicitly defined for each configuration in order to execute the simulation. Energy usage for data collection, UUV travel and data transmission are included in the simulation. Delivery delays for individual data packets are tracked as well as the visit times of each UUV to each data collection node location. Multiple delay metrics are evaluated. The simulation provides highly accurate results, but requires a high computation cost. Thus we perform high-fidelity simulation evaluations only for selected topology configurations based on the results of the low-fidelity models. We verify the consistency of the results over different topology configurations, for example, that the configurations that produce shorter revisit times using the low-fidelity

models also produce shorter revisit times using the high-fidelity models, thus demonstrating the utility of low-fidelity and high-fidelity models for topology optimization problems.

2 TOPOLOGY DESIGN PROBLEM DESCRIPTION

This paper focuses on the scenario of a 100 km^2 plot of ocean for an underwater environment survey. The design concept is to use UUVs to collect data packets from locations called data collection nodes, and transport the data to a depot node, where the data is transmitted from the UUV to the depot and then ultimately sent to a decision location. This scenario example considers that each UUV has on-board sonar capability to collect an image of the area represented by the data collection node. This environment survey data is referred to as a data packet, and is of constant size. In the future, we will consider data collection nodes that accumulate data packets continuously and relay data to neighboring nodes.

In this paper, data collection nodes are placed uniformly 1 km apart in a 10-by-10 grid across the 100 km^2 area, as in Figure 1. UUVs start from and return to a single depot node to charge and deliver data.

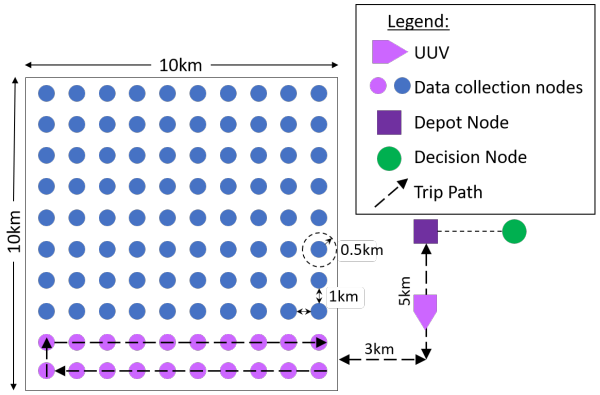

Figure 1: 10-by-10 fixed grid data collection node layout with an example city-block trip path, starting and ending at the purple depot node for data delivery and UUV recharging.

We assume that all nodes are visited by at least one UUV, and when multiple UUVs are available, the workload (number of data collection nodes to visit) is evenly balanced. For the low-fidelity model we assume a worst-case travel time computed using a city-block path for all UUVs according to the path shown in Figure 1. In this way defining the number of UUVs in use and the number of nodes that each UUV visits, which is uniform across UUVs by the assumption of balanced workloads, provides a complete description of the configuration. In the high-fidelity simulation, specific UUV paths are followed to each node location in an efficient manner (see Figure 4).

There is one additional key component of these configurations that is worth defining explicitly for each configuration, namely the "coverage," which captures redundancy. The coverage is defined as the total percentage of nodes visited by all UUVs. It is assumed that, similar to balancing UUV workloads, node coverage is also balanced. As such, a configuration with 100% coverage has each node visited by a single UUV, while a configuration with 200% coverage has each node visited by two UUVs. As another example, a configuration with 320% coverage has every node visited by at least three UUVs: 20% of the nodes are visited by a fourth UUV, with the remaining 80% of nodes visited by exactly three UUVs.

A set of 33 configurations with number of UUVs ranging from 1 to 5 and coverage ranging from 100% to 500% is listed in Table 1. Two example configurations are shown in Figure 2. The number of data collection nodes serviced by each UUV is varied by 10 nodes at a time. A case with 100% coverage, such that every node is serviced without redundancy, was evaluated for each number of UUVs as a base case. In order to achieve as close as possible to 100% coverage in the case of 3 UUVs, each UUV visits 33 nodes,

and in the case of 4 UUVs, each UUV visits 25 nodes (configurations 8 and 16 in Table 1, respectively). The last two columns of Table 1 are metrics calculated with the low-fidelity model (see Section 3).

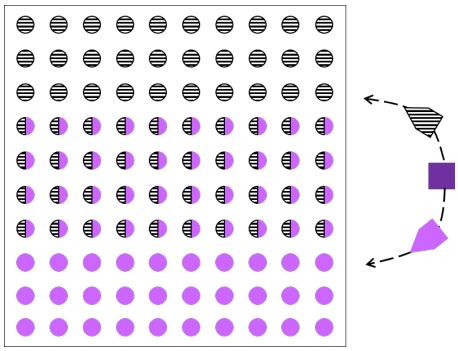

(a) Configuration with 2 UUVs servicing 70 nodes each and 140% coverage (configuration 4 from Table 1).

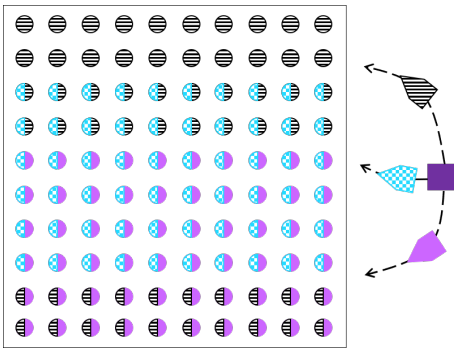

(b) Configuration with 3 UUVs servicing 60 nodes each and 180% coverage (configuration 11 from Table 1).

Figure 2: Two example configurations of nodes visited by UUVs. Each pentagon shaped UUV services the nodes of their corresponding color and pattern. The purple square represents the depot.

Several parameters that specify the scenario are listed in Table 2. These parameter values are inferred from the findings provided in a report as part of the study to support the Powering the Blue Economy Initiative by the U.S. Department of Energy (LiVecchi et al. 2019). A UUV travels at a constant speed and makes a round-trip from the depot, visiting up to two rows of data collection nodes (the maximum without risk of exhausting its battery). The UUV then delivers data to the depot via an optical link and recharges its battery at the depot. The UUV energy usage is modeled by three parameters: travel energy usage, data collection energy usage at node locations, and data transmission energy usage to depot.

3 LOW-FIDELITY MODEL DEVELOPMENT

The low-fidelity model makes simplifying assumptions and aggregates details into group representations. In the low-fidelity model, a 20-node trip length between battery charges is assumed for the purposes of calculating reliability and latency metrics. Path planning is not considered in the low-fidelity model.

In a 10-by-10 fixed grid of data collection nodes, a 20-node trip is an intuitive trip length as this involves traveling across one row of nodes and then traveling back to the depot via another row. This 20-node trip, including the travel distance to and from the depot, is a total of 36 km as measured by a city-block method (see Figure 1). This provides the distance for a worst-case path and is used as the travel distance for every trip in the low-fidelity model.

Based on the parameter values in Table 2 for travel energy usage, data collection energy usage, and battery capacity, a round trip of 36 km and data collection at 20 nodes will drain 3800 kJ. Based on the battery charging rate, it will take 2.64 hours to recharge the 3800 kJ of energy drained in one trip. Based on the UUV travel speed, the 36 km trip takes 5 hours. Data transmission to the depot node will occur simultaneously with charging and will not increase the time the UUV is at the depot node. The total time per trip (travel time plus recharge time) is therefore 7.64 hours.

3.1 Probabilistic Reliability Model

Given that there is inherent uncertainty in the data collection and delivery process, such as transmission interference and the possibility of UUV or sensor mechanical malfunction, reliability must be considered when making decisions on configurations.

Table 1: List of 33 design configurations and results.

#	# of UUVs	Config. Coverage	# of Nodes Covered by Different # of UUVs					# Nodes Serviced per UUV	Weighted Average Revisit Time (hr)	Expected # Unsuccessful Deliveries
			1	2	3	4	5			
1	1	100%	100	0	0	0	0	100	38.19	43.30
2	2	100%	100	0	0	0	0	50	19.10	43.30
3	2	120%	80	20	0	0	0	60	20.63	38.39
4	2	140%	60	40	0	0	0	70	21.39	33.48
5	2	160%	40	60	0	0	0	80	21.39	28.57
6	2	180%	20	80	0	0	0	90	20.63	23.66
7	**2**	**200%**	**0**	**100**	**0**	**0**	**0**	**100**	**19.10**	**18.75**
8	3	99%	99	0	0	0	0	33	12.48	42.87
9	3	120%	80	20	0	0	0	40	13.75	38.39
10	3	150%	50	50	0	0	0	50	14.32	31.02
11	3	180%	20	80	0	0	0	60	13.75	23.66
12	3	210%	0	90	10	0	0	70	12.92	17.69
13	3	240%	0	60	40	0	0	80	13.24	14.50
14	3	270%	0	30	70	0	0	90	13.18	11.31
15	**3**	**300%**	**0**	**0**	**100**	**0**	**0**	**100**	**12.73**	**8.12**
16	4	100%	100	0	0	0	0	25	9.55	43.30
17	4	120%	80	20	0	0	0	30	10.31	38.39
18	4	160%	40	60	0	0	0	40	10.69	28.57
19	4	200%	0	100	0	0	0	50	9.55	18.75
20	4	240%	0	60	40	0	0	60	9.93	14.50
21	4	280%	0	20	80	0	0	70	9.80	10.24
22	4	320%	0	0	80	20	0	80	9.68	7.20
23	4	360%	0	0	40	60	0	90	9.74	5.36
24	**4**	**400%**	**0**	**0**	**0**	**100**	**0**	**100**	**9.55**	**3.52**
25	5	100%	100	0	0	0	0	20	7.64	43.30
26	5	150%	50	50	0	0	0	30	8.59	31.02
27	5	200%	0	100	0	0	0	40	7.64	18.75
28	5	250%	0	50	50	0	0	50	7.96	13.43
29	5	300%	0	0	100	0	0	60	7.64	8.12
30	5	350%	0	0	50	50	0	70	7.80	5.82
31	5	400%	0	0	0	100	0	80	7.64	3.52
32	5	450%	0	0	0	50	50	90	7.73	2.52
33	**5**	**500%**	**0**	**0**	**0**	**0**	**100**	**100**	**7.64**	**1.52**

Table 2: Parameters for scenario specification.

Parameter	**Value**
Travel energy usage	100 J/m
Data collection energy usage	10 kJ/node
Battery charging rate	400 J/s
UUV travel speed	2 m/s

Let the probability of successful data collection by a UUV at a data collection node be p_s, let the probability of a UUV successfully completing a round-trip to the depot be p_u, and the probability of successful transmission of all data packets collected by a UUV to the depot be p_g. Assume that these probabilities are the same for any UUV and data collection node and all events are independent. With these assumptions, the counting process for successes (or failures) of the overall data collection system is modeled as a binomial process.

Consider a single UUV visiting 20 locations on a single round-trip to the depot. The probability that i out of 20 data packets get successfully delivered to the depot by a single UUV is,

$$P(i \text{ successful deliveries out of 20 by one UUV}) = \begin{cases} \binom{20}{i} p_s^i (1-p_s)^{20-i} p_u p_g & \text{for } i = 1,\ldots,20 \\ 1 - p_u p_g (1-(1-p_s)^{20}) & \text{for } i = 0. \end{cases}$$

It follows from the binomial distribution that the expected number of data packets, out of 20, that are successfully delivered to the depot by one UUV on one trip is

$$E[\text{successful deliveries out of 20 by one UUV}] = 20 p_s p_u p_g.$$

Depending on the configuration of UUVs, some data collection nodes may be visited by more than one UUV allowing for improved reliability through UUV redundancy. Suppose that k UUVs make independent trips to visit a set of nodes. To simplify the analysis, we express the probability that a data packet from a single data collection node is successfully delivered to the depot by at least one of the k UUVs, as

$$p_d^{k\text{-shared}} = 1 - (1 - p_s p_u p_g)^k.$$

Using a binomial distribution, it follows that the expected number of successful deliveries out of 20 nodes by at least one of k UUVs can be written as

$$E[\text{successful deliveries out of 20 nodes by } k \text{ UUVs}] = 20 p_d^{k\text{-shared}} = 20(1-(1-p_s p_u p_g)^k).$$

The expected number of unsuccessful deliveries out of 20 nodes, or in other words, the expected number of data collection nodes that fail to have their data successfully transmitted to the depot, can be written as

$$E[\text{failed deliveries out of 20 nodes by } k \text{ UUVs}] = 20 - 20(1-(1-p_s p_u p_g)^k) = 20(1-p_s p_u p_g)^k.$$

Considering the field of 100 data collection nodes and any configuration in Table 1, let r_k be the number of nodes serviced by k UUVs (where $0 \le r_k \le 100$ and $\sum_{k=1}^{5} r_k = 100$), and n be the number of nodes serviced by each UUV (where $0 \le n \le 100$). For each configuration, the values r_k for $k = 1,\ldots,5$ are in columns 4-8 of Table 1, and n appears in column 9 of Table 1. The expected number of nodes that are not delivered to the depot by any of the k UUVs can be written as

$$E[\text{failed deliveries out of 100 nodes for a configuration}] = \sum_{k=1}^{5} r_k (1-p_s p_u p_g)^k. \tag{1}$$

In the low-fidelity model results, we used parameter values of $p_s = 0.9$, $p_u = 0.7$, and $p_g = 0.9$ based on expert opinion. A sensitivity analysis was performed by varying values for p_s, p_u, and p_g. The results are discussed in the last paragraph of Section 3.3. It was observed that changing these values did not impact the optimal configuration determined for each number of UUVs.

3.2 Latency Model

For the environmental survey operation scenario considered in this paper, there are two main metrics to consider when quantifying latency: data latency and revisit time. Data latency is the elapsed time between when a data packet is collected at the data collection node and when it is delivered to the depot. For this scenario (as described in Section 2), the data is collected when a UUV visits the data collection location and is then delivered to the depot at the completion of one trip. This means that the data latency is directly related to the trip time. Since path planning is ignored in the low-fidelity model, this metric does not distinguish configurations. As such, the low-fidelity model focuses on revisit time. Revisit time at a data collection node is defined as the time between consecutive visits from UUVs at that node. In the case that a node is visited by multiple UUVs, it is assumed that the time between UUV visits are evenly spaced. It is also assumed that each UUV visits the same number of data collection nodes. Therefore the revisit time at a data collection node is simply the total time (travel plus recharge time) each UUV spends visiting its set of data collection nodes divided by the number of UUVs that visit that data collection node.

For a configuration with k UUVs, n nodes serviced by each UUV, and r_k nodes serviced by k UUVs, for $k = 1,\ldots,5$ (as in Table 1), we calculate the weighted average revisit time, denoted T, as the sum of the revisit time for each number of UUVs visiting a single data collection node, denoted T_k, multiplied by the proportion of data collection nodes in the configuration with that number of UUVs, i.e.,

$$T = \sum_{k=1}^{5} \left(\frac{r_k}{100} T_k \right), \text{ where } T_k = \left(7.64 \frac{n}{20} \right) / k. \tag{2}$$

Note that the number of trips each UUV takes is the number of data collection nodes serviced by that UUV divided by 20, and the time for each trip is 7.64 hours.

3.3 Low-Fidelity Model Results and Findings

The expected number of failed completions (as defined in (1) in Section 3.1), and the weighted average revisit time (as defined in (2) in Section 3.2), are calculated for each of the 33 configurations. These calculations were performed in a Microsoft Excel spreadsheet and the computational time was nearly instantaneous. These two metrics appear in columns 11 and 12 of Table 1, and are plotted in Figure 3.

An optimal configuration minimizes both the weighted average revisit time and the expected number of failed completions. Notice that the two metrics are not in conflict. More specifically, configurations with the same number of UUVs have similar revisit times while increased coverage significantly reduces the expected number of unsuccessful completions.

As can be seen in Figure 3, there is a clear efficient frontier of optimal configurations. When only one UUV is available, there is only one possible configuration, namely configuration number 1 (see Table 1), and this point is dominated by all other points. When the number of UUVs ranges from 2 to 5, there is a single configuration that dominates the others with the same number of UUVs. Specifically, configurations 7, 15, 24, and 33, for 2, 3, 4, and 5 UUVs, respectively, are optimal. It can be noted that the case with 100% coverage and the case with maximum redundancy for each number of UUVs have the same revisit time, which is an intuitive result. The low-fidelity model also supports the intuition that maximizing redundancy increases reliability without sacrificing revisit time.

A larger number of UUVs allows for lower revisit times and lower number of unsuccessful deliveries. The improvement in revisit time and reliability is detailed in Table 3. The marginal improvement of each additional UUV decreases with each additional UUV. The number of UUVs can be considered as a measure of cost, demonstrating a clear trade-off between the number of UUVs used in the configuration and the resulting revisit time and reliability.

Given a fixed number of UUVs, it should be noted that the decrease in reliability with less coverage (90 nodes versus 100 nodes per UUV) is small. This means that if it is extremely difficult to ensure maximum

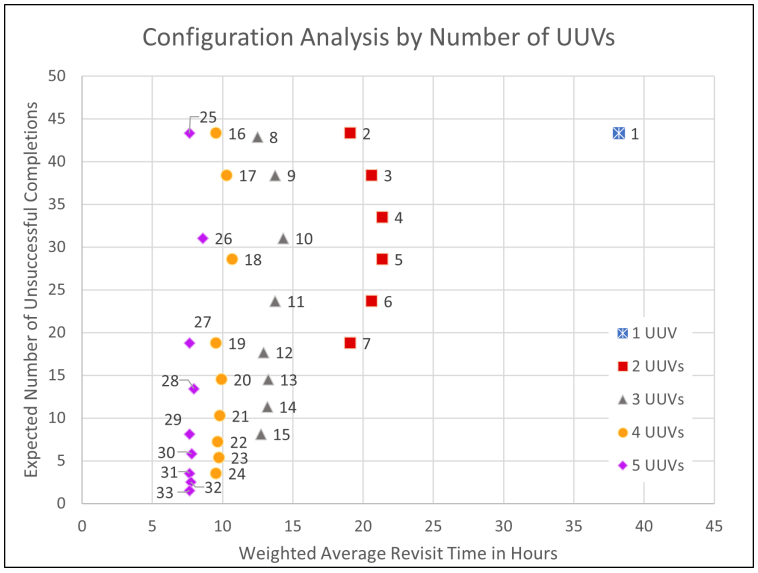

Figure 3: Plot of reliability and latency metrics for different numbers of UUVs. The data labels (positioned near each point) correspond to configuration numbers in Table 1.

redundancy, due to situational constraints outside of the scope of these models such as strong currents or physical obstacles, then a near-optimal configuration can still be achieved.

Sensitivity Analysis: A sensitivity analysis was performed by adjusting the trip time from within the range of 1 to 20 hours (baseline of 5 hours) and charge time within the range of 0.5 to 10 hours (baseline of 2.64 hours). The probability of successful data collection (p_s), trip completion (p_u), and packet transmission (p_g) were adjusted as well within the range of 0.25 to 0.95 (baseline of 0.9, 0.7, and 0.9, respectively). Changing these five parameters impacted the metrics proportionally for all configurations. Under all combinations tested, the optimal configurations were consistent. This sensitivity analysis revealed that the results identified above are robust.

4 HIGH-FIDELITY SIMULATION DEVELOPMENT

The high-fidelity simulation was developed in the Network Simulator NS-3 (NS-3 Consortium 2021) using the Underwater Acoustic Network (UAN) module. The data collection nodes are laid out in the same 10-by-10 grid pattern described in Section 2. The UUVs move according to a waypoint mobility model, with a waypoint specified each time they change direction. The waypoints are selected such that the UUVs traverse directly over top of the data collection nodes in straight line paths. An "arrival" radius of 25 m is defined for each node such that once a UUV is within this radius it generates a data packet to represent the sonar image at that location. These packets are stored on the UUV in a queue until the UUV returns to the depot, at which point they are successively transmitted to the depot using a simulated data link. The UUVs are each staggered by two minutes at the start of the simulation such that even if they traverse identical length paths they do not arrive at the depot at the same time and thus packet collisions are avoided. After each trip, the UUV returns to the depot to deliver the collected packets and recharge its battery. A battery model is leveraged to track the energy remaining in the UUV as it travels. Energy is used for propulsion according to the rate specified in Table 2 as well as for the data communications according to a modem energy model for transmit, receive, and idle time. The recharge time required at the depot is computed based on the energy level remaining upon returning and the recharge rate specified in Table 2. After recharging is completed, the UUV is assigned a new path and it once again traverses the assigned nodes in the field.

Table 3: Marginal improvement metrics of lowest revisit time and lowest unsuccessful deliveries.

# UUVs	Lowest Revisit Time	# Improvement vs. 1 UUV	% Improvement vs. 1 UUV	# Improvement vs. Previous	% Improvement vs. Previous
1	38.19	N/A	N/A	N/A	N/A
2	19.10	19	49.99%	19	49.99%
3	12.73	25	66.67%	6	33.35%
4	9.55	29	74.99%	3	24.98%
5	7.64	31	79.99%	2	20.00%

# UUVs	Lowest Unsuccessful Deliveries	# Improvement vs. 1 UUV	% Improvement vs. 1 UUV	# Improvement vs. Previous	% Improvement vs. Previous
1	43.30	N/A	N/A	N/A	N/A
2	18.75	25	56.70%	25	56.70%
3	8.12	35	81.25%	11	56.69%
4	3.52	40	91.87%	5	56.65%
5	1.52	42	96.49%	2	56.82%

Unlike the low-fidelity model, specific paths for the UUVs for each configuration are created in the simulation. Seven configurations corresponding to one, two, and five UUVs were simulated, as shown in Table 4. The one- and five-UUV cases used the same assumption as the low-fidelity model, where the UUV was assigned to traverse two adjacent rows at a time and then return to the depot, followed by another set of two rows, etc. For the two-UUV cases, the field was divided approximately in quarters as shown in Figure 4 in order to avoid partial paths where a UUV would traverse an area without collecting any data; two of the paths contain 24 nodes and the other two contain 26. All UUV paths in the high-fidelity simulation also differ from that of the low-fidelity in terms of including shortest length (diagonal) legs to get between the depot and the sensor field as opposed to the city block assumption since this would be a more realistic pattern for UUVs to traverse in order to minimize time and energy usage.

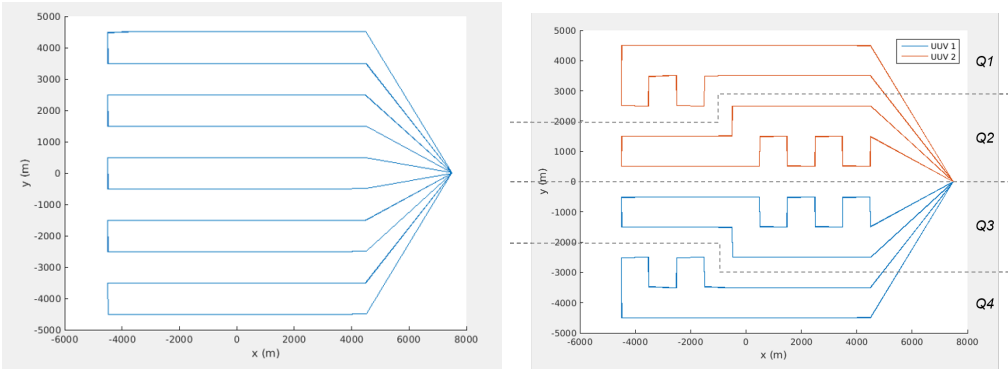

Figure 4: Plots of the UUV paths in the high-fidelity simulation for the cases where a single UUV covers 100 nodes with 20 nodes per path (left), and the case where two UUVs split the nodes (right) and the field is divided in quarters (Q1 - Q4).

Table 4: High-fidelity simulation results.

#	# of UUVs	Config. Coverage	# of Nodes Covered by Different # of UUVs				# Nodes Serviced per UUV	Avg Pkt Latency (hr)	Revisit Time (hr)			Exec Time (sec)
			1	2	3	5			Avg.	Min	Max	
1	1	100%	100	0	0	0	100	1.90	28.28	28.21	28.36	9
2	2	100%	100	0	0	0	50	2.23	13.60	13.59	13.63	13
4.5	2	150%	50	50	0	0	75	2.23	13.36	6.66	20.35	14
7	2	200%	0	100	0	0	100	2.23	13.56	6.66	20.53	13
25	5	100%	100	0	0	0	20	1.89	5.63	5.22	6.11	44
29	5	300%	0	0	100	0	60	1.89	5.62	0.21	10.64	45
33	5	500%	0	0	0	100	100	1.89	5.65	5.27	6.10	45

4.1 High Fidelity Simulation Results and Findings

A summary of the revisit time and packet latency metrics for the high-fidelity simulation are shown in Table 4. Note that the second two-UUV case does not exactly map to a configuration number of the low-fidelity model, due to the fact that the field was split into quarters instead of 20-node sections in order to make the UUV routing more efficient, and thus falls half-way between configurations 4 and 5 in terms of allocations of nodes serviced.

It is observed that the average node revisit time is nearly identical for each set of cases for the same number of UUVs, but intuitively, decreases with more UUVs that service the field since more trips are then concurrently executed. This is consistent with the low fidelity results, although the exact numbers vary due to the detailed modeling of UUV path length and recharge time in the high fidelity simulation. In addition to the average revisit time, the minimum and maximum revisit times for each node are captured. These are additional factors from the high-fidelity simulation that may be considered when choosing a configuration not defined in the low-fidelity model. For example, from the low-fidelity model it was concluded that the maximum redundancy configuration was optimal to minimize revisit time and expected number of unsuccessful deliveries. The high-fidelity simulation with specific path planning for routing of UUVs demonstrates a larger revisit variance. As discussed in more detail later, revisit time is most uniform for the case of no redundancy and potentially increases in variance with more complex allocations of nodes to UUVs, depending on how routes are chosen.

An additional metric, that of packet latency from generation time until the time it is delivered to the depot, is available from the high-fidelity simulation. This is observed to be entirely dictated by the path of UUVs employed; the 1-UUV and 5-UUV cases each have 20 nodes per trip, while the 2-UUV cases have (on average) 25 nodes per trip and exhibit a larger latency.

While the average interval between node visits for the three 2-UUV and the three 5-UUV cases are nearly identical, the variance of revisit times, as seen by the minimum and maximum revisit times, is impacted by the UUV routing plan. Example histograms for revisit time per node in the 5-UUV cases are shown in Figure 5. In the 100% coverage case, three different revisit times are observed due to the differing distances from the depot to the nodes in rows being serviced, with nodes in rows 1-2 and 9-10 experiencing the longest revisit times, while rows 3-4 and 7-8 experiencing moderate revisit times, and rows 5-6 experiencing the shortest revisit times. A similar phenomenon is observed for the 500% coverage case, except that a cyclic pattern is experienced as the UUVs rotate through different trip lengths over the set of 5 path pairs visited, which results in four dominant revisit times. For the middle case of 300% coverage (configuration 29), the cumulative trip and recharge times result in a large variance of node revisit times. In this situation, sometimes all of the UUVs are visiting independent rows while sometimes they end up visiting the same two rows in close succession while others are not serviced.

Though the histograms for the 2-UUV cases are not shown due to space limitations, variations are observed due to the order in which quarters of the field are visited. For the 150% coverage configuration

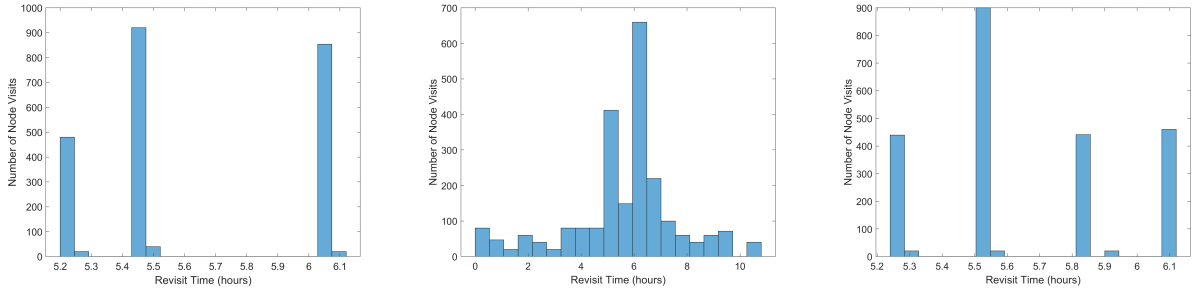

Figure 5: Histograms of the revisit times for each node for each UUV trip for the three different 5-UUV configurations: 100% coverage (left), 300% coverage (center), and 500% coverage (right).

4.5, one UUV visits Q1, Q2, Q3 and repeats, while the other visits Q4, Q3, Q2 and repeats. Due to this specific path planning, the nodes in Q1 and Q4 have a gap of 2 trips between visits, while nodes in Q2 and Q3 are visited sequentially and then have a gap of only 1 trip. For the 200% coverage configuration 7, one UUV visits the quarters from top to bottom (Q1, Q2, Q3, Q4, repeat) while the other visits from bottom to top. This results in different revisit times per node. This further demonstrates that path planning impacts revisit time variances. The variance in revisit times may influence the decision of optimal configuration.

The computation time of each simulation run is listed in the final column of Table 4. It should be noted that this is just one implementation of a "high fidelity" simulation, and the execution time can be greatly affected by how the modeling is chosen to be done. For example, the UUV mobility model is simplistic and does not account for deviations due to ocean currents or other disturbances. The time horizon for the simulation runs was 136 hours. This was chosen to allow approximately 24 round trips of the UUVs. The length of the time horizon impacts computation time. For comparison, one high-fidelity simulation run ranged from 9 to 45 seconds while the low-fidelity model computation time is essentially instantaneous for all 33 configurations.

5 CONCLUSION AND FUTURE WORK

This paper focuses on the development of a multi-fidelity approach to handle a multi-objective optimization problem. The approach was implemented around a maritime environmental survey operation scenario using multiple UUVs, as defined in Section 2, where data packets are collected upon arrival of the UUV to a data collection location. This scenario has allowed for the demonstration of the optimization approach, where the low-fidelity models is used to identify potential optimal configurations for a given number of UUVs that can then be evaluated by the high-fidelity simulation.

The low-fidelity model in Section 3 provides a measure of reliability and shows that redundancy greatly reduces the expected number of nodes with unsuccessful deliveries. The expected revisit times calculated with the low-fidelity model do not show much difference for configurations, but is consistent with the finding that configurations with maximum redundancy are optimal.

The high-fidelity simulation in Section 4 validates the conclusion that configurations with maximum redundancy are optimal, however, the simulation provides insight into the impact of path planning on performance. Additional measures not calculated in the low-fidelity model, such as packet latency and the minimum and maximum revisit times, can also be gathered by the simulation. In this way, the low-fidelity models can evaluate many different configurations and identify the most promising, and then the high-fidelity simulation can provide additional data on those configurations to assist in more informed decision making.

Future work will include a method of incorporating packet generation failures and UUV failures into the high-fidelity simulation, to account for reliability of a given configuration. In addition, we will consider fixed sensors at data collection nodes that accumulate data packets continuously. The number of data packets collected by a UUV will depend on the time of the last collection. Future work will also consider different

modes of communications, such as optical and acoustic communication, with different ranges, reliability, and data rates. The existence of cross-links between sensor nodes will be considered allowing for data to be accumulated at certain nodes. The methods introduced in this paper may be expanded to additional metrics of the topology optimization problem, such as network connectivity and lifetime, prioritization, and energy consumption. The methods introduced in this paper may be expanded to include air, land, and space communications.

ACKNOWLEDGMENTS

This work has been funded, in part, by the Office of Naval Research and the Naval Information Warfare Center Pacific.

REFERENCES

Echeveste, D., A. Lee, and N. Clark. 2021. "Using Spatial Uncertainty to Dynamically Determine UAS Flight Paths". *J Intell Robot Syst* 101.

Fletcher, B. 2000, September. "UUV master plan: a vision for navy UUV development". In *Proceedings of the OCEANS 2000 MTS/IEEE Conference and Exhibition*, 65–71. Providence, Rhode Island: IEEE.

Fu, M. C. 2015. *Handbook of Simulation Optimization*. Springer.

Kang, Y., L. Mathesen, G. Pedrielli, and F. Ju. 2017. "Multi-fidelity modeling for analysis of serial production lines". In *Proceedings of the 2017 13th IEEE Conference on Automation Science and Engineering (CASE)*, 30–35. Xi'an, China: IEEE.

Linz, D. D., H. Huang, and Z. B. Zabinsky. 2017, December. "Multi-fidelity simulation optimization with level set approximation using probabilistic branch and bound". In *Proceedings of the 2017 Winter Simulation Conference*, edited by W. K. V. Chan, A. D'Ambrogio, G. Zacharewicz, N. Mustafee, G. Wainer, and E. Page, 2057–2068. Las Vegas, NV: Institute of Electrical and Electronics Engineers, Inc.

LiVecchi, A., A. Copping, D. Jenne, A. Gorton, R. Preus, G. Gill, R. Robichaud, R. Green, S. Geerlofs, S. Gore, D. Hume, W. McShane, C. Schmaus, and H. Spence. 2019, April. "Powering the Blue Economy; exploring Opportunities for Marine Renewable Energy in Maritime markets". Technical report, U.S. Department of Energy, Office of Energy Efficiency and Renewable Energy, Washington, D.C.

NS-3 Consortium 2021. "Network Simulator NS-3 Consortium". https://www.nsnam.org/ accessed on Feb. 15, 2021.

Vasilescu, I., K. Kotay, D. Rus, M. Dunbabin, and P. Corke. 2005. "Data Collection, Storage, and Retrieval with an Underwater Sensor Network". In *Proceedings of the 3rd International Conference on Embedded Networked Sensor Systems*, SenSys '05, 154–165. New York, New York: Association for Computing Machinery.

Zhang, Z., and Z. Fei. 2007. "Route Design for Multiple Ferries in Delay Tolerant Networks". In *Proceedings of the 2007 IEEE Wireless Communications and Networking Conference*, 3462–3467: IEEE.

Zwolak, K., B. Simpson, B. Anderson, E. Bazhenova, R. Falconer, T. Kearns, H. Minami, J. Roperez, A. Rosedee, H. Sade, N. Tinmouth, R. Wigley, and Y. Zarayskaya. 2017, June. "An unmanned seafloor mapping system: The concept of an AUV integrated with the newly designed USV SEAKIT". In *Proceedings of OCEANS 2017 - Aberdeen*. Aberdeen, UK.

AUTHOR BIOGRAPHIES

Danielle Morey is a graduate student in the Department of Industrial and Systems Engineering at the University of Washington, with a BSISE from Ohio State University. Her email address is dmorey43@uw.edu.

Cherry Wakayama is a research scientist in the Intelligence, Surveillance and Reconnaissance Department at Naval Information Warfare Center Pacific. Her research interests include applications of operations research for maritime operations. Her email address is cherry.wakayama@navy.mil.

Randall Plate is an electrical engineer in the Intelligence, Surveillance and Reconnaissance Department at Naval Information Warfare Center Pacific. He works in the areas of underwater and atmospheric acoustics, and modeling and simulation. His email address is rplate@spawar.navy.mil.

Zelda Zabinsky is a Professor in the Department of Industrial and Systems Engineering at the University of Washington. She is an INFORMS Fellow and an IISE Fellow. Her email address is zelda@uw.edu. Her website is https://ise.washington.edu/facultyfinder/zelda-zabinsky.